

The impact of ACL laxity on a bicondylar robotic knee and implications in human joint biomechanics

Felix Russell, Petar Kormushev, Ravi Vaidyanathan, Peter Ellison

Abstract—Objective: Elucidating the role of structural mechanisms in the knee can improve joint surgeries, rehabilitation, and understanding of biped locomotion. Identification of key features, however, is challenging due to limitations in simulation and in-vivo studies. In particular the coupling of the patello-femoral and tibio-femoral joints with ligaments and its impact on joint mechanics and movement is not understood. We investigate this coupling experimentally through the design and testing of a robotic sagittal plane model.

Methods: We constructed a sagittal plane robot comprised of: 1) elastic links representing cruciate ligaments; 2) a bi-condylar joint; 3) a patella; and 4) actuator hamstrings and quadriceps. Stiffness and geometry were derived from anthropometric data. 10° – 110° squatting tests were executed at speeds of 0.1 – 0.25 Hz over a range of anterior cruciate ligament (ACL) slack lengths.

Results: Increasing ACL length compromised joint stability, yet did not impact quadriceps mechanical advantage and force required for squat. The trend was consistent through varying condyle contact point and ligament force changes.

Conclusion: The geometry of the condyles allows the ratio of quadriceps to patella tendon force to compensate for contact point changes imparted by the removal of the ACL. Thus the system maintains a constant mechanical advantage.

Significance: The investigation uncovers critical features of human knee biomechanics. Findings contribute to understanding of knee ligament damage, inform procedures for knee surgery and orthopaedic implant design, and support design of trans-femoral prosthetics and walking robots. Results further demonstrate the utility of robotics as a powerful means of studying human joint biomechanics.

I. INTRODUCTION

The knee is the largest synovial joint in the human body [1]. Its role is critical in bipedal locomotion and knee joint damage often necessitates major surgery and/or extensive rehabilitation to restore even partial mobility. The femur and tibia, central to the structure of the knee, make contact with each other at the tibio-femoral joint through smooth surfaces called condyles. These surfaces slide and roll over each other as the joint rotates and are held together by four ligaments. In addition

the patella (knee cap) rests on the posterior surface of the femoral condyle forming the patello-femoral joint. The patella is attached to both the quadriceps muscle group and the tibia via tendons such that contraction of the quadriceps applies force to the patella, which in turn extends the knee joint during locomotion [1]. Despite its critical role in human movement, precise understanding of how the patello-femoral and tibio-femoral joints work as a system has yet to be fully explained in the literature. Such understanding is vital to improve our comprehension of the interaction of the internal elements of the human knee, which is necessary to improve the outcome of joint surgeries [2]. It is well known that damage to structures such as ligaments can change joint kinematics, for example, changing the location and variance of the axis of rotation [3]. It is also known that those who suffer from loss of ligaments such as the anterior cruciate ligament (ACL) still retain some joint function [4], [5]. A subset of these patients are able to adapt their gait such that they can continue to perform high impact tasks such as hopping and running [5], [6] despite significant changes in static joint laxity and gait kinematics. Although, reconstructive surgery is able to restore gait kinematics to be closer to that of healthy individuals [7], the reconstructed side is 3 times more likely to be affected by mechanical degradation of the joint surfaces caused by changes in mechanical stress - termed osteoarthritis [8]. A deeper understanding of these joint mechanisms can lend critical insights into joint degradation. Furthermore, insights gained into the mechanics of the human knee have useful applications in the design of trans-femoral prosthetic knees for amputees and joint designs for walking (legged) robots.

A range of tools have been introduced to study knee biomechanics with the goal of interpreting aspects of joint performance. Video fluoroscopy, for example, has been implemented to compare the kinematics of joints that have been resurfaced with those of healthy individuals. Findings demonstrate that joints where more of the ligaments are retained but the joint surfaces are replaced do not always restore kinematics to that of the healthy joint [9], [10]. Further fluoroscopic studies on healthy individuals show that the interaction between the ligaments and the tibio-femoral kinematics is complex and a large amount of any result is affected by the patient and the test conditions [11], [12]. As the patella cannot be accurately tracked using fluoroscopy these studies typically focus on the tibio-femoral joint, which neglects the importance of the patello-femoral joint on the function of the knee. Additionally, neither fluoroscopy or the more commonly used tracking cameras allow any direct measure of the forces being imparted on the internal structures of the joint. This necessitates

Manuscript received August, 2019; revised December, 2019. This work has been supported by the UK Engineering and Physical Sciences Research Council (EPSRC) and UK Medical Research Council (MRC) Confidence in Concept (CiC) Scheme with Össur inc.

Felix Russell is with the Biomechanics Lab, Department of Mechanical Engineering, at Imperial College London, London, UK. Ravi Vaidyanathan is with the Biomechanics Lab, Department of Mechanical Engineering and the UK Dementia Research Institute-Care Research and Technology Centre, Imperial College London, London, UK. E-mail: felix.russell12@imperial.ac.uk and r.vaidyanathan@imperial.ac.uk. Petar Kormushev is with the Robot Intelligence Lab at the Dyson School of Design Engineering, Imperial College London, London, UK. E-mail: p.kormushev@imperial.ac.uk. Peter Ellison is at the Department of Orthopaedic Surgery, Haukeland University Hospital and Department of Clinical Medicine, University of Bergen both in Bergen, Norway. E-mail: peter.ellison@outlook.com

computer models to estimate muscle forces from the available measurements [13]. Obvious human subject considerations limit interventions to study the mechanical performance of the knee. For example, it is not possible to study movement impact of changing a single variable (e.g. ligament tension) through a range of values during walking.

Cadaver studies are commonly used to bridge this knowledge gap [14]–[16]. For example, to improve the outcome of reconstructive surgeries, a cadaveric knee from a healthy subject is manipulated in-vitro to estimate the degree of post-surgery tension in the reconstructed ligament that a surgeon should aim for [17]. Investigations have demonstrated that low final tension will lead to excessive joint laxity [18]. Conversely there is evidence excessive tension is linked to a number of negative outcomes including loss of maximum knee extension [19], [20], increased tibio-femoral compressive forces [21], graft failure [20] and unnatural translation of tibia [16]. It is also theorised that the unnatural translation of the tibia leads to a reduced moment arm of the patella tendon which demands higher quadriceps forces during movement [22].

These have lent crucial understanding the importance of ligaments within the joint and surgical reconstruction. However, the use of cadavers makes it difficult to observe the total effect of interventions on the movement of the joint when all the elements, patella, joint surface and ligaments interact under dynamic conditions at physiological loads and speeds. This is partly because mechanical properties of cadaveric tissue degrades and due to difficulties applying loads to tissue. Therefore, cadaver studies are typically done in static or quasi-static test conditions without dynamic forces, which obfuscates full understanding. Also large amounts of variation between limited supplies of cadaveric samples can make resulting data noisy. The separation of the joint from the whole leg system can also lead to unrealistic loading conditions.

The goal of our ongoing work is to understand the dynamic interaction between the knee cruciate ligaments, patello-femoral joint and condyles over a range of test conditions comparable to regular human movement. This necessitates experimental models with the capacity to create physiologically similar ligament and tendon forces as well as joint velocities generated in locomotion. It further demands tests that can be executed under tightly controlled conditions such that the effect of changing a single variable (e.g. ACL length/tension) can be quantified. Achievement of this aim required a different approach to the in-vivo and cadaveric techniques common in contemporary literature. In this investigation, we introduce an anthropomorphic robotic sagittal plane model of the knee complete with elastic ligaments with adjustable slack length. This allows the execution of systematic tests in order to understand the basic underlying principals of knee joint motion when subject to physiological loads. In addition we are able to directly measure system variables such as actuator forces and ligament lengths which is not possible in human or cadaver studies.

A. Related Work

While robotic testing apparatuses have been fabricated to perform dynamic testing on cadaver samples, robotic systems

directly simulating knee behaviour are rare. Our novel system draws in part from mechanisms used in cadaveric studies and mathematical models of knee locomotion. In comparison with systems used specifically for cadaveric studies, our anthropomorphic platform shares characteristics with the Kansas/Purdue II knee simulator. This 5 controllable degree of freedom hydraulic squatting simulator [23] operates under force control in the vertical axis at the hip and adduction-abduction axis at the ankle. There is torque control in the vertical and flexion axes at the ankle and position control on an actuator simulating the quadriceps. This system has primarily been used with cadavers to validate computational models [24]–[26]. The motivation for our work is to elucidate key features of the mechanics of the joint itself and, in particular, the role of the ligaments and patella in joint function. Sagittal plane mathematical models have been used in the investigation of the knee biomechanics in previous studies [27]–[29] and validated against measurements from fluoroscopic techniques [30]. With this in mind we build a simplified sagittal plane mechanical model of the joint with elastic ligaments, patella and joint surfaces to systematically investigate the mechanical relationship between the different joint elements.

A smaller body of work has investigated robotic replication of the human knee to study its mechanical efficiency. The joint itself has several advantages which can be exploited by muscles for control [31], which potentially outstrip current robotic joints. Simple mechanisms have implemented a pin joint and cam [32], [33] and synthesised four bar mechanisms to achieve the desired motion [34], [35] while more complex designs have drawn on knee joint structures for human augmentation [36]. Collectively these investigations have captured features of knee joint kinematics, stiffness or moment arm. More physiologically driven studies [37], [38] implemented a robotic system based on condylar knee design with demonstrated mechanical benefits, though tendons or compliance were not

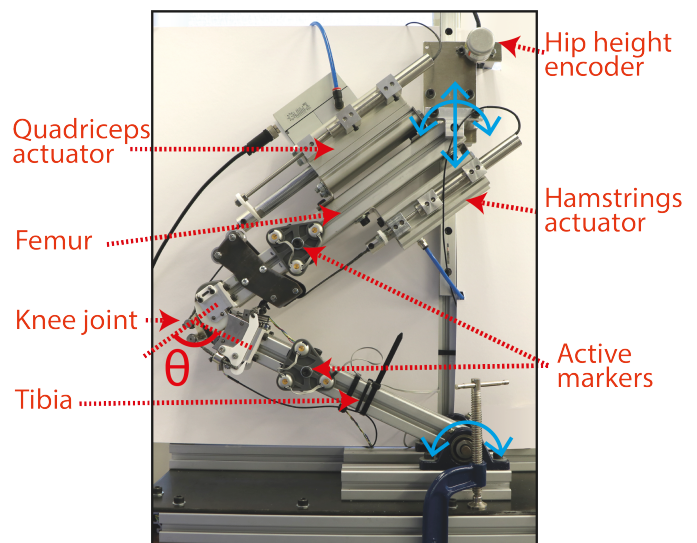


Figure 1: Robotic knee squatting test setup, shown here at the maximum flexion angle of 117° . The external degrees of freedom are marked in blue.

directly investigated. Our own work on human-like knee joints [39]–[41] explored similar issues for the purpose of designing new joints for walking robots or exoskeletons. The patella was simplified as a bracket attached to the tibia or pulley attached to the femur in those studies. The location of this bracket was selected in order to replicate, in simulation, the moment arm of the patella tendon [40]. We found that this does not, however, produce the realistic joint loads required to study the fundamental mechanics of the human knee joint. To address these shortcomings the robotic model described in this paper has been designed and improved. Joint geometries are much closer to those found in human knees and a floating patella is added; the system hardware includes larger actuators able to impart higher forces that better match physiological values and additional sensors are incorporated to measure actuator length. The resulting test platform allows unique testing to elucidate knee joint biomechanics.

B. Aims and Objectives

In this study we aim to understand the dynamic interaction between the patella, condyles and cruciate ligaments in the human knee when subjected to dynamic loads. In order to achieve this we perform automated tests and observe how the system kinematics respond to changes in ACL slack length. The tests are performed on a biologically accurate robotic sagittal plane model of the human knee joint. During these tests we use a number of sensors to record:

- 1) Force in the elastic ligaments
- 2) Contact point of the femoral condyle on the tibial condyle
- 3) Quadriceps mechanical advantage
- 4) Quadriceps force

We aim to use this information, in addition to still images taken of the robot at various points in its motion to understand:

- 1) The role of the patello-femoral joint for the robustness of the knee system as a whole when subject to the removal of the ACL.
- 2) The effect of ligament tension on joint function.

II. METHODS

The overall test setup (see figure 1) consists of a mechanical model of the knee joint (described in Section II-A) attached to beams representing the tibia and femur. The tibia is pinned at the ankle with a single rotational degree of freedom in the sagittal plane. The ‘hip’ consists of a rotational degree of freedom in the sagittal plane and a translational degree of freedom in the vertical direction.

Movement in the joint is controlled by two pneumatic actuators representing the quadriceps and hamstrings muscle groups. A proportional pressure valve allows the controller to continually update the actuator forces. The maximum forces for the quadriceps and hamstrings are 1.68 kN and 249 N , respectively. The hip is unloaded (other than by the weight of the vertical sled itself) so we were able to use actuators that could generate around a quarter of those estimated in-vivo in maximally loaded humans [42]. We found that the quadriceps

actuator reached maximum forces of 1.4 kN during testing. The smaller actuator size allowed us to keep the weight of the system down and improved the resolution of the force control, both of which facilitated higher testing speeds.

The actuators are attached to Dyneema[®] (ultra high molecular weight polyethylene) cord, representing tendons. The material was chosen for its high strength and stiffness (17.6 kN and 3.5% elongation at breaking load) and the ability for it to pass round smaller radius pulleys than the equivalent steel cable. The cord is routed through pulleys so that lines of action of the forces matches those found in humans (see figure 2). The antagonistic actuator (i.e. the muscle being extended) is set to provide a constant 30 N force. The precise amount of co-contraction present in-vivo is uncertain [43] so in this study we follow previous in-vitro squatting studies that employ constant co-contraction forces of between 10 N and 90 N [14], [15], [43], [44]. Pilot tests showed that whilst increasing the level of co-contraction increased the hysteresis like movement of the knee, the overall trends observed did not change. 30 N was selected for this study as it provided a good balance between stability (seemingly provided by higher antagonistic forces) and the risk of hyperextension which occurred when the ACL spring was removed and the antagonistic force was too high. The actuators are fitted with displacement transducers in parallel. An encoder at the hip provides information on the absolute position of the joint for feedback to the controller.

Active markers fixed to the femur and tibia are tracked using an NDI Certus Optotrack system in order to provide measurements of joint position. The markers emit infrared light that the camera can detect. The known layout of the three markers on each joint allows the joint angle and translation to be calculated. The marker mounts are designed to bolt directly onto slots in the aluminium extrusion that makes up the femur and tibia. This ensures that there is good alignment between the axes of the marker and those of joint segments. The camera has a 3D accuracy of 0.1 mm and cameras of this type have been found to be suitable for similar kinematic studies [45].

A. Joint geometry

The joint (see figures 2 and 3) consists of two joint surfaces, condyles, that slide and roll over each other as the joint rotates, held together by elastic ligament analogues. A patella analogue is attached to the quadriceps actuator and the tibia. The patella position was selected using the MRI overlay of a normal adult male human knee shown in figure 2.

The femoral joint surface is a sagittal plane slice of the femur bone scan taken by Isaza et al. [47], simplified into three arcs (see figure 2). The tibial surface is then generated using a kinematic model of the joint system in order to ensure smooth contact between the surfaces. This model uses a relationship between the ligament lengths and angles taken from studies on cadavers [48], [49]. The ligament attachment points are from Fuss et al. [50]. Multiple sources are used since no single source contained all the information required to build the joint. The design process for the joint surfaces has been described in previous work by the authors [41].

Ligament stiffness is provided by linear non-viscoelastic springs with stiffness 126 Nmm^{-1} , similar to that found by

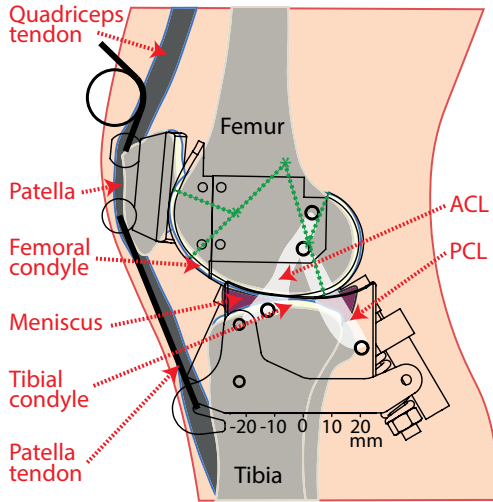


Figure 2: The robotic joint and patella layout compared to a trace of a sagittal plane MRI of the human knee. The meniscus and tibial condyle are combined for the purposes of the robotic joint. The MRI used can be found at [46].

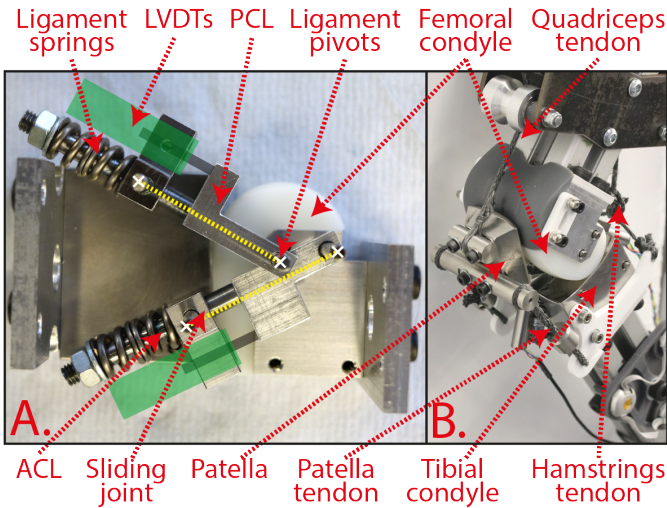


Figure 3: The anthropomorphic knee joint shown in cross-section (A) and in position on the squatting test rig (B). Linear variable differential transformers (LVDTs) are used to measure the ligament length. The position of these elements is shown in green. The nuts allow the slack or free length of the ligaments to be changed. A smaller slack length means that the ligament is tighter and vice versa

Jones et al. [51] in humans. The patella size is taken from an MRI study by Yoo et al. [52] and the shape from Baldwin et al. [53]. The lengths and positions of the cables, representing tendons, are chosen to match an MRI scan of the human knee (see figure 2)

B. Test protocol

The ligament slack lengths are adjusted using a nut on each ligament. A single revolution of the nut is known to change the length by 1 mm. A test protocol was performed at each

ACL length. A fully automated method was chosen to reduce random error in the test results. The following is performed in sequence for each of the test conditions.

- 1) Bedding in: 2 full range cycles are performed initially so that the joint positions can adjust to the new ligament stiffness. After adjustment of ligament slack lengths the measured variables such as ACL length were observed to stabilise to a single path as a function of angle (i.e. reaching a dynamic equilibrium) after less than half a cycle in all cases.
- 2) Dynamic tests: 6 cycles of $10^\circ - 100^\circ$ at three different speeds. Cycle periods of 10, 7 and 4 seconds were chosen. The system is found to reach a dynamic equilibrium within a quarter of a single cycle after a speed change. Data is therefore not recorded for the first of each set of six to ensure consistency. This is similar to 5 seconds squats used in in-vivo studies [54].
- 3) Static tests: 5 tests at each of 90° , 60° , 30° , 10° , 5° and 0° degrees. The joint is moved at $10^\circ s^{-1}$ between each joint position. At each static angle the set point angle is maintained for 6 seconds to allow the system to settle. The data is collected over the final 0.25 seconds of this period.
- 4) Gait test: 6 cycles are performed with a tibio-femoral flexion-extension profile similar to that found by LaFortune et al. [55]. The cycles are shifted by 10 degrees in the flexion direction so that the range is from 10° to 70° . This is necessary because the knee controller uses hip height to estimate knee angle for feedback into the controller. At 0° this estimate becomes inaccurate and it is not possible to perform good quality control. The cycle is also slowed down so that each cycle is 4 seconds rather than 1.1 seconds. Human gait harnesses the natural dynamics of motion to swing the leg, which facilitates faster cycles. In squat this is not possible and the cycle period has to be increased.

C. Data processing

The joint angles and positions are recorded by an NDI Certus Optotrack camera at 200 Hz. The camera software allows the position and orientation of the marker on the tibia to be given in the reference frame of the femur. The actuator forces are inferred from the measured pressure at the output of the pressure regulator. The ligament forces are calculated using the ligament lengths recorded using the inbuilt LVDTs (see figure 3), the known position of the tensioning nut and with the assumption that the compression springs are linear.

1) *Quadriceps mechanical advantage*: The quadriceps mechanical advantage (MA) is the ratio of change in actuator length to change in tibia angle. This calculation gives the MA for the whole patella-quadriceps-joint system. It is calculated by equation (1) where r_k is the quadriceps MA at sample k , L is the actuator length and θ is the joint flexion angle.

$$r_k = \frac{\delta L}{\delta \theta} = \frac{L_{(k-\Delta)} - L_{(k+\Delta)}}{\theta_{(k-\Delta)} - \theta_{(k+\Delta)}} \quad (1)$$

When the change in angle between samples is small, i.e. when joint speeds are small, the equation does not behave

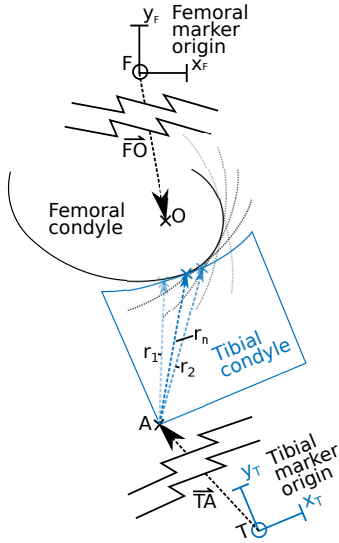


Figure 4: Calculation of the contact point between the femur and tibia. At each sample of joint position a golden Section search, r_1 to r_n , is performed to find the point where the distance between the surfaces is minimised. The vectors $\vec{F}\vec{O}$ and $\vec{T}\vec{A}$ are calibrated so that the average overlap at the contact point between the surfaces is minimised across all angles

well. This is therefore only recorded for the cases when the magnitude of joint velocity is greater than $20^\circ s^{-1}$

2) *Contact point*: The positions of the tibial condyle surface in the reference frame of the femur is found using standard coordinate transformations and measurements from the robot and CAD models of the joint. The contact point can then be found as the point of smallest distance between the two condyles (see figure 4). This is done using a golden-section search along the surface of the tibial profile. To calibrate the system the measured vectors $\vec{F}\vec{O}$ and $\vec{T}\vec{A}$ are adjusted so that the average distance at contact between the two joint surfaces is minimised across all angles. This calibration is done using the MATLAB interior point minimiser. It is only necessary to perform this calibration once after setup.

3) *Instantaneous centre of rotation (ICR)*: The centre of rotation at these angles is found by evaluating the change in position of the tibia marker (T in Figure 4) over a $0.1 s$ time period. The radius of curvature is then found with (2).

$$\rho = \frac{\delta x}{\delta \theta} \quad (2)$$

The location of the centre of rotation is then a distance ρ in the direction perpendicular to δx . This is then used in the calculation of moment arm described in Section II-D.

D. Quasi-static tests

In order to help explain the results found in the tests described above a separate quasi-static test was performed with the aim of understanding how the direction of the forces and the length of the moment arm changed with ACL slack.

In this test the joint motion is controlled so that it moves with a slower sinusoidal period of 30 seconds. A digital camera

with a macro lens is used to take an image when the joint passed through each of 4 angles, 15° , 30° , 60° and 90° when moving in the flexion direction. The correct moment to take the image is shown visually on the controlling computer. This is performed with the ACL both at the tightest setting of $31.94 mm$ and with the spring removed.

For these tests the ratio of quadriceps force to the patella tendon force is found from the force balance on the patella. In addition, the moment arm of the patella tendon is found as the perpendicular distance from the patella tendon to the instantaneous centre of rotation. We also calculate the expected mechanical advantage, as seen by the quadriceps, by finding the product of these two variables.

Additionally a separate test is conducted to find the ligament forces at full extension. The commanded joint angle is slowly reduced from 5° flexion towards 0° and the ligaments forces are recorded at the points at which it passes through 0.

III. RESULTS

A. Ligament forces

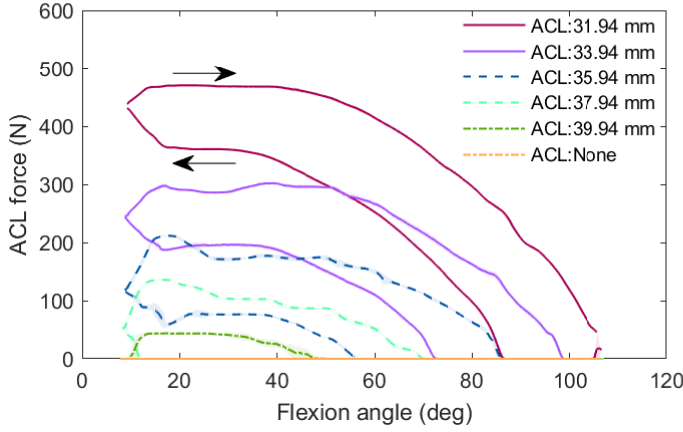
Figure 5 shows that ACL forces are higher in extension and lower in flexion, and that the opposite is true for the PCL. The forces are also higher when the joint is moving in the flexion direction for the ACL and in the extension direction for the PCL. Figure 5 shows that a tighter ACL increases the force on the PCL in extension but makes little difference when the joint is in flexion. The range of angles over which the ACL and PCL are active (forces greater than zero) are both increased by tightening the ACL. The angle at which the ACL transitions from active to inactive (forces equal to zero) increases as the ligament slack length is decreased.

B. Contact point

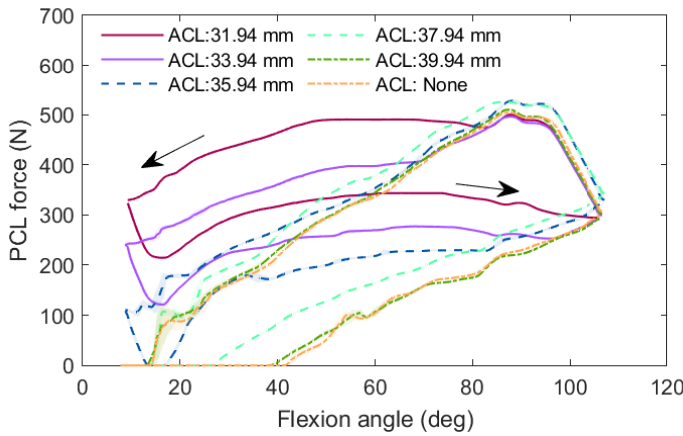
Figure 6 shows that the contact point location is different depending on whether the joint is moving in flexion or extension directions. Between these two states there is a transition. We observed that the contact always transitions between these two lines at the point in motion where the direction change has occurred. Loosening the ACL increases this difference. Figure 6 shows that loosening the ACL moves the contact point posteriorly. When the ACL is inactive, i.e. where the ACL force is zero (see Figure 5), the contact points all follow one common path, moving in the posterior direction with extension (for 120° to 20°) and in the anterior direction with flexion. When the ACL force begins to increase from zero the contact point begins to deviate from this path. The change in slope of the contact point curve when the ACL is loosened affects the amount of slip between the condyles. A negative slope indicates that there is more slipping since pure rolling would manifest itself as the contact point rolling posteriorly as the flexion angle increases.

C. Quadriceps mechanical advantage

Figure 7 shows the mechanical advantage of the quadriceps. The average difference between each line and the mechanical advantage at the median slack length of $35.94 mm$ ranged



(a) ACL force



(b) PCL force

Figure 5: Ligament forces as a function of knee flexion angle and ACL slack length. The shaded area shows the range of values recorded. The arrows show whether motion is in the flexion (to the right) or extension (to the left) directions.

from 0.71 mm to 1.46 mm depending on direction on motion and ACL slack length. This compares to mean standard deviations for each test of between 0.49 mm and 1.50 mm . For the tightest ACL setting of 31.94 mm we see the largest differences of over 15% (10 mm) reduction in mechanical advantage where angles are smaller than 14° and up to 10% (5 mm) reduction where angles are between 15° and 45° .

D. Quadriceps force required for extension

Figure 8 shows the quadriceps actuator force required to perform squat as a function of joint angle and ACL slack length. The average difference between each line and the mechanical advantage at the median slack length of 35.94 mm ranged from 6.9 N to 44.4 N depending on direction of motion and ACL slack length. The average difference was 11.6 N . This compares to mean standard deviations for each test of between 8.9 N and 18.8 N . The largest differences were for movements in the extension direction when the ACL is in the tightest configurations. Here we see quadriceps forces increase with peak changes of 72 N . This effect is more profound

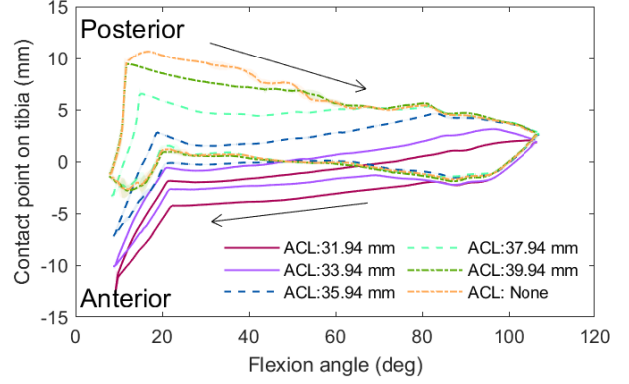


Figure 6: Contact point as a function of knee flexion angle and ACL slack length. The shaded area shows the range of values recorded. The arrows show whether motion is in the flexion (to the right) or extension (to the left) directions.

closer to 0° flexion (see also Section III-E) and there is little difference close to maximum flexion, where the ACL is less active.

E. ACL force at 0 degrees

Figure 9 shows the ligament forces when the joint is at 0 degrees. The ACL tightness increases ACL forces at extension.

F. Effect of speed

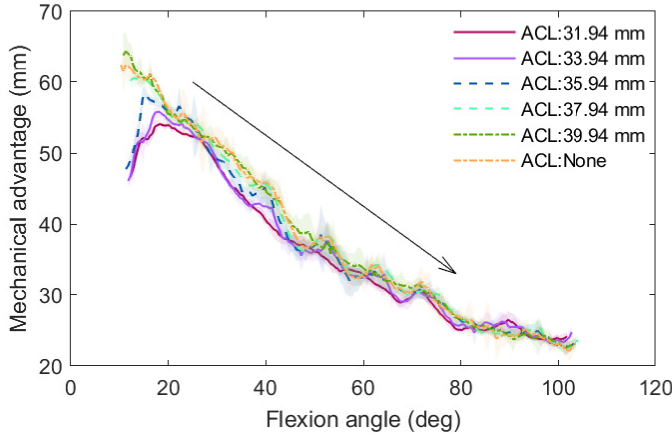
The average difference between the contact points at the different speeds compared to the 7 second period test for each ACL slack length ranged from 0.12 mm to 0.41 mm . This compares to standard deviations of between 0.050 mm and 0.310 mm . Figure 10 shows the plot for the three speeds at two different values of ACL slack length. We also observe that faster speeds reduce the largest flexion angle achieved by 5 mm ($\sigma = 0.71\text{ mm}$). Qualitatively we observe a slight increase in instability with speed, especially when the ligaments are loose. This happens as we approach the maximum achievable accelerations for the control system and can be seen as a higher variance in Figure 10. Throughout the rest of these results we have plotted the 7 second period test.

G. Gait cycle

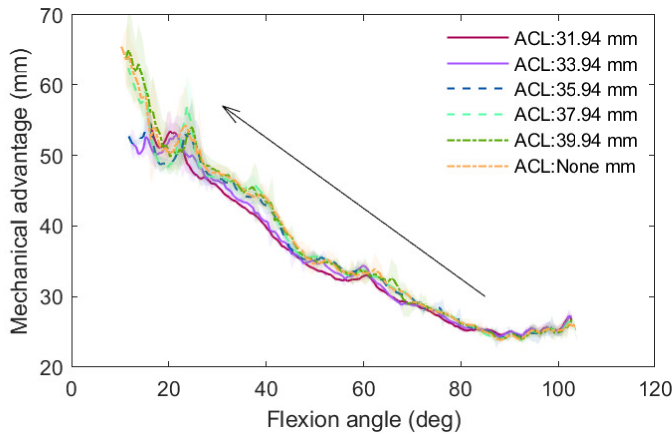
Figure 11 shows that a gait cycle is poorly achieved when the ACL is very slack or the spring is removed. In these cases the first spike in angle, representing stance stage flexion, is not achieved. At the highest ACL tensions the error at the point of maximum flexion angle is increased from 6.1° (with an ACL length of 37.9 mm) to 10.5° (with an ACL length of 31.9 mm).

H. Quasi-static tests

Table I shows the change in the ratio of quadriceps to patella tendon force and moment arm to the instantaneous centre of rotation (ICR) both as a function of ACL state and joint angle. It was also observed that when the ACL was tight the ICR



(a) mechanical advantage moving in flexion direction



(b) mechanical advantage moving in extension direction

Figure 7: Quad Mechanical Advantage ratio as a function of knee flexion angle and ACL slack length. The shaded area shows the range of values recorded. The arrows show whether motion is in the flexion (to the right) or extension (to the left) directions.

remains a smaller distance from the intersection of the two ligaments than when the ACL spring is removed (1.68 mm compared to 5.27 mm).

Table I: Ratio of tendon forces and moment arm for the quasi-static tests on the robotic joint.

Angle	ACL	$\frac{ F_P }{ F_Q }$	Patella tendon moment arm, R	Expected mechanical advantage
15°	31.94 mm	99.2%	51.7 mm	51.3 mm
15°	None	97.2%	57.0 mm	55.4 mm
30°	31.94 mm	97.7%	50.8 mm	49.6 mm
30°	None	92.7%	53.6 mm	49.7 mm
60°	31.94 mm	75.0%	44.2 mm	33.1 mm
60°	None	73.7%	46.8 mm	34.5 mm
90°	31.94 mm	64.8%	40.2 mm	26.0 mm
90°	None	64.6%	40.1 mm	25.9 mm

IV. DISCUSSION

Using a robotic sagittal plane model of the human knee joint we have measured the effect on knee joint dynamics of

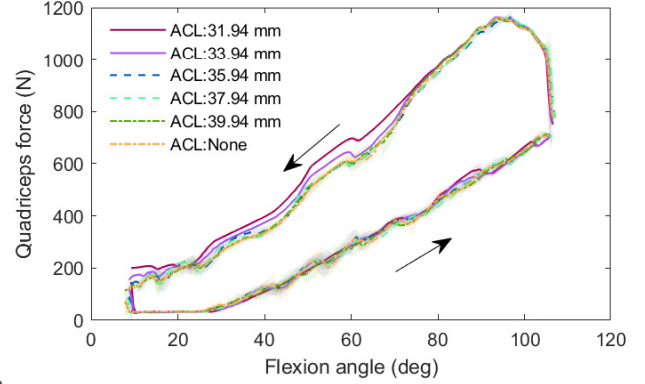


Figure 8: Quadriceps Force as a function of knee flexion angle and ACL slack length. The shaded area shows the range of values recorded. The arrows show whether motion is in the flexion (to the right) or extension (to the left) directions.

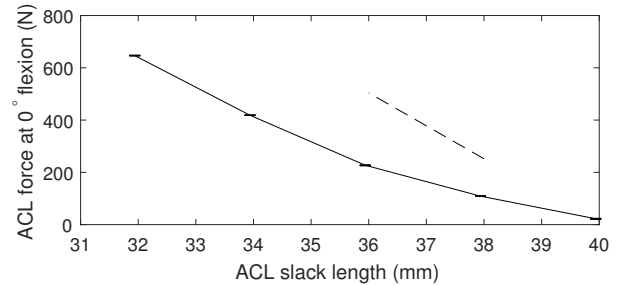


Figure 9: ACL force at 0 degrees flexion (solid line). For comparison a dashed line shows the 126 N/mm force-displacement slope of the ligaments spring.

removing or loosening the ACL. Differently from previous studies [40], [56], [57] we don't use the line of action of the patella tendon, but instead calculate the amount the quadriceps actuator itself has to move for every small rotation of the joint. This allows us to find the total mechanical advantage for the whole mechanism. Our data shows that the change in contact point location is not mirrored by an equal change in the mechanical advantage of the quadriceps (see figure 7) and that there is very little change in the required quadriceps forces (see figure 8). Partly this is because the instantaneous centre of rotation of the system remains close to the flexion facet centre of the femur (FFC labelled in Figure 12). Since the patella moves with the femur, the distance between the patella and FFC is relatively unchanged. This mitigates some of the expected change in mechanical advantage.

The remaining effect comes from changes in the patella position. Figure 12 shows the forces in the patello-femoral joint system. Here we can visualise the three forces on the patella: Two, F_P and F_Q , must act along the tendons and the remaining contact force, F_R , must be perpendicular to the patella surface and pass through the centre of the section of condyle upon which it contacts (assuming a frictionless contact). As these forces are in equilibrium, the ratio of the magnitudes of the quadriceps tendon to patella tendon force can be calculated by balancing the triangle of forces. Table I

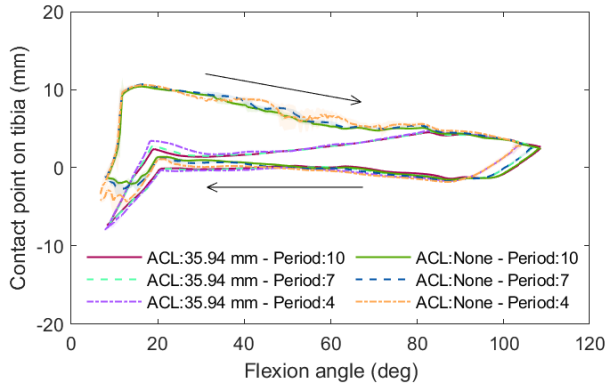


Figure 10: Contact point when the joint is subject to sinusoidal target angles with different periods. The period is given in seconds. The shaded area shows the range of values recorded. The arrows show whether motion is in the flexion (to the right) or extension (to the left) directions.

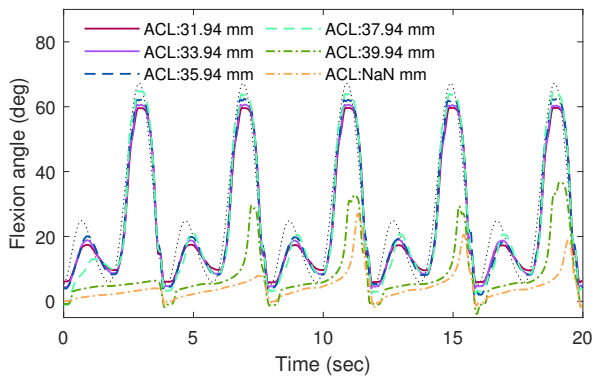


Figure 11: Five gait-like cycles at 4 Hz and different ACL slack lengths. The target angle is shown as a dotted black line.

shows how this ratio changes with angle and ACL tightness. The decrease in this ratio as flexion angle increases is widely reported in the literature [58]. More interestingly we see that the ratio of patella tendon force to quadriceps tendon force reduces when the ACL is removed. This somewhat counteracts the increase in moment arm, R . As the position of the femoral contact point moves posteriorly R increases but the patella is also able to sit higher on the femoral condyle, reducing the angle between the patella tendon and the axis of the tibia. This leads to a reduction in the tendon ratio. The precise nature of this behaviour is controlled by the geometry of the tendons and condyles.

The overall effect is that, except at small flexion angles, ACL tightness has relatively little influence on quadriceps mechanical advantage or the required quadriceps force for a squat. Limited investigation into the effect of PCL slack length was performed on the system described here. More detailed study of the effects of PCL length is a matter for future work. Initial results suggest that, like ACL length, PCL length has very little effect on quadriceps mechanical advantage and required force. Qualitatively the joint stability significantly

reduced when the PCL was very loose or removed which made testing these conditions more challenging than for spring-less ACL.

A. Other effects of ligament tightness

Although the effect of ACL length on mechanical advantage is somewhat mitigated by the patello-femoral joint system we do observe effects on other aspects of joint performance. For example, over-tightening of the ACL significantly increases the ligament forces throughout joint motion (see figure 5), including on the PCL. Particularly large forces are observed in the ACL at full extension when the ligament is tight (see figure 9). It is noteworthy however that without a kinematic response from the system we would expect to see that a 2 mm reduction in ligament slack length would increase ligament forces by 252 N (given the ligament stiffness of 126 Nmm^{-1}). However the changes are always smaller than this, indicating the joint system allows the condyles to move in such a way as to relieve some of this tension. Additionally, when the ACL is shortest we see an increase in the quadriceps force needed for movement in the extension direction but little change in moment arm. This suggests that the extra force is instead required to overcome friction inside the joint or in building up elastic energy within the ligaments to be released upon flexion. An investigation into the contribution of these two factors is beyond the scope of this work.

We also observe that excess ligament length impaired the ability of the controller to perform the rapid flexion near to 0° required during simulated walking (see figure 11). This is, in part, due to the additional hyper-extension available in the joint. This impaired the ability of our controller to estimate joint angle and move the joint into flexion and the knee to lock out. Although our control system is different to that of the human neuromuscular system it is noteworthy that ACL deficient patients do exhibit reduced quadriceps moment and increased hamstring EMG to maintain stability in standing [59]. This suggests that the human knee may be experiencing similar problems from ACL deficiency to those that we observe.

Finally, we observed that although ligament tightness changes the contact point position, direction of joint motion also has a significant effect (see figure 6). The difference in position when moving in each direction can be as much as 10 mm when the ACL is loose. As the ACL is tightened the difference decreases. This highlights the importance of dynamic effects in biomechanical testing, of performing these dynamic tests in both directions and then treating the data separately. With static testing the joint is in the transition between these two states which leads to large variation in the results depending on the direction of approach. This explains why we were unable to achieve reliable results using this test method and should inform future testing protocols.

The ability of the joint to maintain mechanical advantage but with a reduction in stability and a change in joint kinematics is similar to that observed in ACL deficient patients. These patients can still retain some level of joint function [4], [5] and, with adaption of their gait, some are even able to perform high

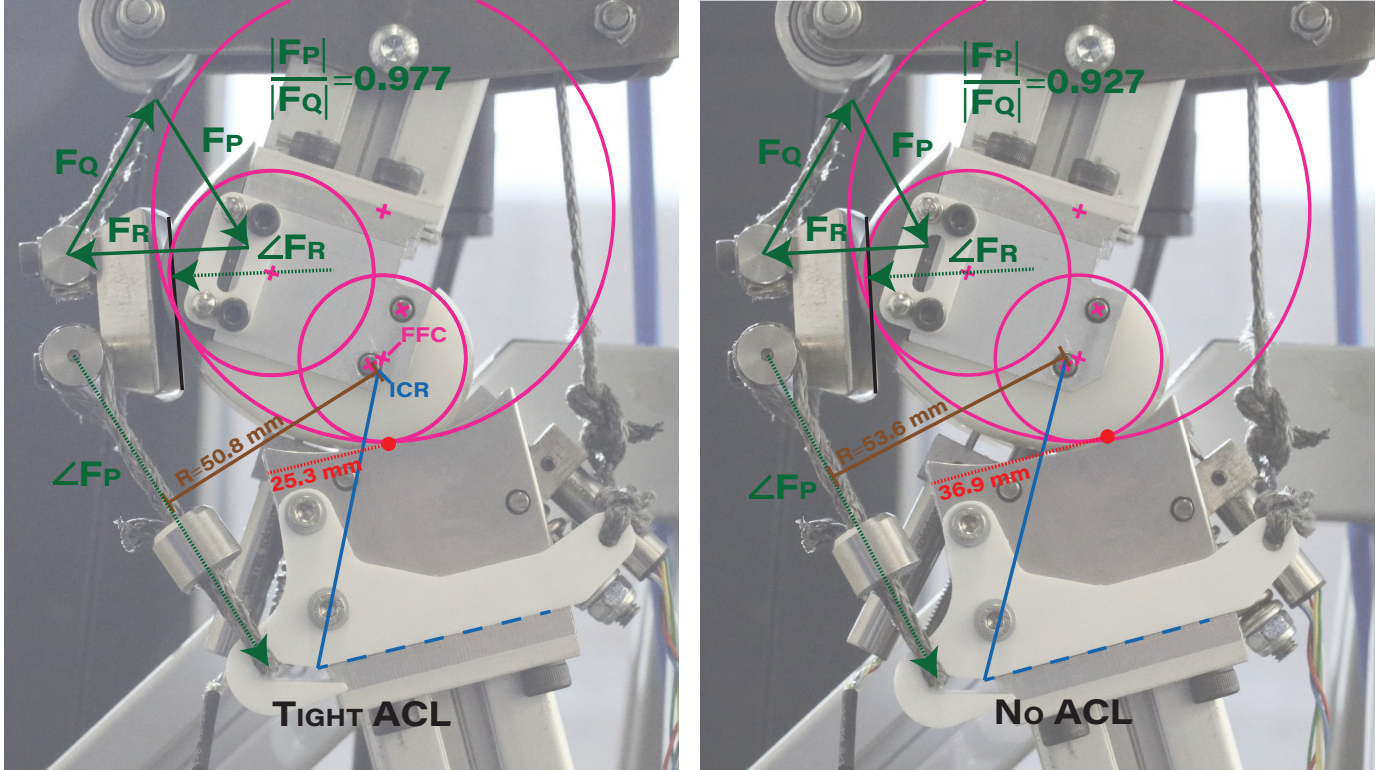


Figure 12: Analysis of the lines of effect of ligament tightness on the moment arm of the quadriceps, an example at 30° . FFC denotes the flexion facet centre, i.e. the centre of the portion of the femur in contact with the tibia through most of the range of motion (shown in magenta). Also marked are the instantaneous centre of rotation (ICR) found using the method described in Section II-C3 (blue); the contact point of the femur on the tibia (red); the moment arm of the patella tendon (brown) and the force balance on the patella (green). $\angle F_R$ and $\angle F_p$ indicate the directions but not magnitude of these forces.

impact tasks such as running or hopping [5], [6] (see Section I).

We found that there was little difference in kinematics between squatting tests run at speeds of 4, 7 and 10 seconds per squat. It is possible that this is a result of including no viscoelasticity in the ligaments (further discussion in section IV-C). All the speeds showed the same overall kinematic interaction of the joint elements that this paper was seeking to investigate with the predominant effect being a slight increase in instability at small angles observed with the 4 second squat. As a result the 7 second squat is shown in the plots which is significantly closer to physiological speeds than many much slower in-vitro studies [15], [43], [44].

Static tests performed using the procedure described in Section II-B were unsuccessful. When settling on the static set point the direction of motion could be either positive or negative at the time at which the data was recorded. The direction of motion has a significant effect on the contact point and ligament forces and, when transitioning between the two directions, the measured values are somewhere between the two (see figures 5 and 6). This effect is a form of hysteresis and meant that there was often inconsistency between results recorded at the same angles for this test.

B. Comparison to prior art

To validate our results we compared the results from the sagittal plane robotic model to those found in the literature from cadaver or in-vivo studies. When compared to studies looking at contact point position in cadavers [9] our model shows a similar trend with a distinct anterior movement in contact point location from 20° towards full extension and a shallower slope throughout the rest of motion. In-vivo experiments [60], [61] show anterior motion of the contact point with extension by 9 mm , similar to our results. Note however that the measurements in these tests have large uncertainties, greater than 12 mm in some cases [60].

Hoshino et al. [16] show that ACL deficiency moves the femur posteriorly relative to the tibia. This is corroborated by cadaver results from Brady et al. [21], who shows that greater ACL tension moves the femur anteriorly relative to the tibia. Both these effects are seen in our results.

Cohen et al. [49] observe anteromedial bundle ACL lengths of $36.9 \pm 2.8\text{ mm}$ at 0° in in-vivo MRI scans which is similar to the $37.1 - 41.6\text{ mm}$ that we observe in our model. For some metrics it is much harder to make a comparison with the literature. For example there are significant practical challenges to achieving accurate in-vivo readings of ligament and muscle force as a function of angle [62] (see Section I).

Overall we find that our system is within the uncertainties

of comparable tests done both in-vivo and in-vitro.

C. Test method

The authors recognise the limitations of the test method presented here. The study is concerned with the effects of gross relative movements of the femur, the tibia, and the patella during dynamic motion. This knee model is lacking the varus-valgus and axial degrees of freedom that are present in the human knee. With this comes the ability to reduce the number of ligaments and actuators required to constrain and control motion. For example the collateral ligaments and other soft structures have been omitted and the many muscle groups that act on the joint have been simplified to just two actuators. The effects of these structures on the gross kinematics is expected to be small [27]. Furthermore, there is evidence that it is the cruciate ligaments that are most important for constraining motion in the sagittal plane [63] and the authors, therefore, believe that our simpler model with patella, condyles and cruciates is sufficient for studying in plane squatting. This is supported by the previous planar models of the knee that have also neglected the collateral ligaments and other soft tissues [23], [27], [28] and the evidence that they are accurate for measures of similar variables to those measured in this study such as patella tendon angle [30] and quadriceps loading [23]. A future more complete model of the joint may include these additional elements and could be paired with a full 3D model of the condyles. This would allow us to explore the role of ligaments in, for example, the screw home mechanism and mediolateral stability of the patella.

Additionally, our ligaments differ from those found in humans. There the force in the cruciates varies across the ligament as different fibre bundles are brought into tension [64]. This means that the stiffness varies as a function of angle. In the current model we capture the overall force in a ligament, something that is challenging to achieve in-vivo where sensors can only be attached to single bundles [65], [66]. However, it does mean that we lose this anisotropic behaviour.

Human ligaments are non-linear which manifests itself as a rapid reduction in stiffness at low strains with linear behaviour over most of the range of strain to failure [51]. This study can be viewed as looking at only the linear section with the low stiffness section modelled as having zero stiffness. It has also been shown in-vitro that ligaments are viscoelastic with stress relaxation of 6% over 18 seconds of cyclic loading [67]. The difference in ligament force between test conditions that we observe is much larger than this (see figure 5) and therefore it is reasonable to omit these time dependant effects. This is reflected in the similarity between our system and human studies described in Section IV-B.

V. CONCLUSION

We have built a robotic sagittal plane model of the human knee and tested it under conditions of human loading. Experimental results generate new insights as to the role of ligaments and the patella within the robotic model. The role of ACL tension is highly relevant for total knee replacement surgery, where the ACL or both the ACL and PCL are removed.

Furthermore, ACL tension is also significant in ACL reconstruction where the tension of the reconstructed ligament can vary significantly between surgeons. We show that a reduction in ACL tightness, or complete removal of ACL spring force, has no effect on the quadriceps' mechanical advantage or the force required to perform squats, despite changes to tibio-femoral contact point and ligament forces. Our analysis also shows that the patello-femoral joint moves with the tibio-femoral joint. This movement causes the ratio of tensions in the quadriceps to patella tendons to change, which mitigates against any effect on quadriceps mechanical advantage from the change in contact point. Despite the mechanical advantage being maintained, we observe that the stability of the knee is compromised and activities that require small flexion angles, such as a healthy walking gait, become too unstable to be performed. This is similar to observations in ACL deficient humans. These findings uncover critical features of human knee biomechanics. The results contribute to understanding knee ligament damage and how surgeries can improve patient outcomes. The results also provide a new basis for the use of anthropomorphic joint robotic models to study features of human joint biomechanics that cannot be examined in cadaveric or human studies. Finally, elucidating the role of the quadriceps mechanical advantage and its relationship with ligament forces lends insights into the design of new robotic joints for leg amputees or walking robots.

REFERENCES

- [1] C. Sinnatamby, *Last's Anatomy: Regional and Applied*, 12th Edition. Churchill Livingstone/Elsevier, 2011, ISBN: 9780702033940.
- [2] M. A. Roussot and F. S. Haddad, "The evolution of patellofemoral prosthetic design in total knee arthroplasty: How far have we come?", *EFORT open reviews*, vol. 4, no. 8, pp. 503–512, 2019.
- [3] D. A. Dennis *et al.*, "In vivo determination of normal and anterior cruciate ligament-deficient knee kinematics", *Journal of biomechanics*, vol. 38, no. 2, pp. 241–253, 2005.
- [4] T. P. Andriacchi and C. O. Dyrby, "Interactions between kinematics and loading during walking for the normal and ACL deficient knee", *Journal of biomechanics*, vol. 38, no. 2, pp. 293–298, 2005.
- [5] K. S. Rudolph *et al.*, "Dynamic stability in the anterior cruciate ligament deficient knee", *Knee surgery, sports traumatology, arthroscopy*, vol. 9, no. 2, pp. 62–71, 2001.
- [6] K. Rudolph *et al.*, "Dynamic stability after ACL injury: Who can hop?", *Knee Surgery, Sports Traumatology, Arthroscopy*, vol. 8, no. 5, pp. 262–269, 2000.
- [7] B. Shabani *et al.*, "Gait knee kinematics after ACL reconstruction: 3D assessment", *International orthopaedics*, vol. 39, no. 6, pp. 1187–1193, 2015.
- [8] B. Barenus *et al.*, "Increased risk of osteoarthritis after anterior cruciate ligament reconstruction: A 14-year follow-up study of a randomized controlled trial", *The American journal of sports medicine*, vol. 42, no. 5, pp. 1049–1057, 2014.

- [9] S. Fantozzi *et al.*, “Femoral rollback of cruciate-retaining and posterior-stabilized total knee replacements: In vivo fluoroscopic analysis during activities of daily living”, *Journal of orthopaedic research*, vol. 24, no. 12, pp. 2222–2229, 2006.
- [10] W. C. Jacobs *et al.*, “Retention versus removal of the posterior cruciate ligament in total knee replacement: A systematic literature review within the cochrane framework”, *Acta orthopaedica*, vol. 76, no. 6, pp. 757–768, 2005.
- [11] K. Nagai *et al.*, “The complex relationship between in vivo ACL elongation and knee kinematics during walking and running”, *Journal of Orthopaedic Research*, 2019.
- [12] S. S. Jordan *et al.*, “The in vivo kinematics of the anteromedial and posterolateral bundles of the anterior cruciate ligament during weightbearing knee flexion”, *The American journal of sports medicine*, vol. 35, no. 4, pp. 547–554, 2007.
- [13] L. Saccares *et al.*, “A novel human effort estimation method for knee assistive exoskeletons”, in *2017 International Conference on Rehabilitation Robotics (ICORR)*, IEEE, 2017, pp. 1266–1272.
- [14] R. C. More *et al.*, “Hamstrings - an anterior cruciate ligament protagonist: An in vitro study”, *The American journal of sports medicine*, vol. 21, no. 2, pp. 231–237, 1993.
- [15] D. L. Churchill *et al.*, “The transepicondylar axis approximates the optimal flexion axis of the knee”, *Clinical Orthopaedics and Related Research®*, vol. 356, pp. 111–118, 1998.
- [16] Y. Hoshino *et al.*, “The effect of graft tensioning in anatomic 2-bundle acl reconstruction on knee joint kinematics”, *Knee Surgery, Sports Traumatology, Arthroscopy*, vol. 15, no. 5, pp. 508–514, 2007.
- [17] S. L. Sherman *et al.*, “Graft tensioning during knee ligament reconstruction: Principles and practice”, *JAAOS-Journal of the American Academy of Orthopaedic Surgeons*, vol. 20, no. 10, pp. 633–645, 2012.
- [18] S. J. Nicholas *et al.*, “A prospectively randomized double-blind study on the effect of initial graft tension on knee stability after anterior cruciate ligament reconstruction”, *The American journal of sports medicine*, vol. 32, no. 8, pp. 1881–1866, 2004.
- [19] J. C. Austin *et al.*, “Loss of knee extension after anterior cruciate ligament reconstruction: Effects of knee position and graft tensioning”, *JBJS*, vol. 89, no. 7, pp. 1565–1574, 2007.
- [20] C.-J. Wang *et al.*, “Effects of knee position, graft tension, and mode of fixation in posterior cruciate ligament reconstruction: A cadaveric knee study”, *Arthroscopy: The Journal of Arthroscopic & Related Surgery*, vol. 18, no. 5, pp. 496–501, 2002.
- [21] M. F. Brady *et al.*, “Effects of initial graft tension on the tibiofemoral compressive forces and joint position after anterior cruciate ligament reconstruction”, *The American journal of sports medicine*, vol. 35, no. 3, pp. 395–403, 2007.
- [22] J. Suggs *et al.*, “The effect of graft stiffness on knee joint biomechanics after ACL reconstruction—a 3D computational simulation”, *Clinical biomechanics*, vol. 18, no. 1, pp. 35–43, 2003.
- [23] L. P. Maletsky and B. M. Hillberry, “Simulating dynamic activities using a five-axis knee simulator”, *Journal of Biomechanical Engineering*, vol. 127, no. 1, pp. 123–133, 2005.
- [24] K. H. Bloemker *et al.*, “Computational knee ligament modeling using experimentally determined zero-load lengths”, *The open biomedical engineering journal*, vol. 6, p. 33, 2012.
- [25] C. K. Fitzpatrick *et al.*, “Mechanics of post-cam engagement during simulated dynamic activity”, *Journal of Orthopaedic Research*, vol. 31, no. 9, pp. 1438–1446, 2013.
- [26] C. W. Clary *et al.*, “The influence of total knee arthroplasty geometry on mid-flexion stability: An experimental and finite element study”, *Journal of biomechanics*, vol. 46, no. 7, pp. 1351–1357, 2013.
- [27] H. Gill and J. O’Connor, “Biarticulating two-dimensional computer model of the human patellofemoral joint”, *Clinical biomechanics*, vol. 11, no. 2, pp. 81–89, 1996.
- [28] T. W. Kernozek and R. J. Ragan, “Estimation of anterior cruciate ligament tension from inverse dynamics data and electromyography in females during drop landing”, *Clinical biomechanics*, vol. 23, no. 10, pp. 1279–1286, 2008.
- [29] K. Shelburne and M. Pandy, “Determinants of cruciate-ligament loading during rehabilitation exercise”, *Clinical biomechanics*, vol. 13, no. 6, pp. 403–413, 1998.
- [30] B. Van Duren *et al.*, “Approximation of the functional kinematics of posterior stabilised total knee replacements using a two-dimensional sagittal plane patellofemoral model: Comparing model approximation to in vivo measurement”, *Computer methods in biomechanics and biomedical engineering*, vol. 18, no. 11, pp. 1191–1199, 2015.
- [31] S. R. Chang *et al.*, “A muscle-driven approach to restore stepping with an exoskeleton for individuals with paraplegia”, *Journal of neuroengineering and rehabilitation*, vol. 14, no. 1, p. 48, 2017.
- [32] A. G. Steele *et al.*, “Development of a bio-inspired knee joint mechanism for a bipedal robot”, in *Conference on Biomimetic and Biohybrid Systems*, Springer, 2017, pp. 418–427.
- [33] T. Kikuchi *et al.*, “Bioinspired knee joint for a power-assist suit”, *Journal of Robotics*, vol. 2016, p. 1, 2016.
- [34] Y. Asano *et al.*, “Achievement of twist squat by musculoskeletal humanoid with screw-home mechanism”, in *2013 IEEE/RSJ International Conference on Intelligent Robots and Systems*, IEEE, 2013, pp. 4649–4654.
- [35] S. Pfeifer *et al.*, “An actuated transfemoral prosthesis with optimized polycentric knee joint”, in *Biomedical Robotics and Biomechatronics (BioRob), 2012 4th IEEE RAS & EMBS International Conference on*, IEEE, 2012, pp. 1807–1812.

- [36] W. Huo *et al.*, “Impedance reduction control of a knee joint human-exoskeleton system”, *IEEE Transactions on Control Systems Technology*, 2018.
- [37] A. C. Etoundi *et al.*, “A bio-inspired condylar hinge joint for mobile robots”, in *Intelligent Robots and Systems (IROS), 2011 IEEE/RSJ International Conference on*, IEEE, 2011, pp. 4042–4047.
- [38] A. Etoundi *et al.*, “A bio-inspired condylar hinge for robotic limbs”, *ASME Journal of Mechanisms and Robotics*, vol. 5, no. 3, pp. 1–8, 2013.
- [39] F. Russell *et al.*, “Challenges in using compliant ligaments for position estimation within robotic joints”, in *Rehabilitation Robotics (ICORR), 2017 IEEE International Conference on*, IEEE, 2017.
- [40] F. Russell *et al.*, “A biomimicking design for mechanical knee joints”, *Bioinspiration & biomimetics*, vol. 13, no. 5, p. 056012, 2018.
- [41] F. Russell *et al.*, “A kinematic model for the design of a bicondylar mechanical knee”, in *2018 7th IEEE International Conference on Biomedical Robotics and Biomechatronics (Biorob)*, IEEE, 2018, pp. 750–755.
- [42] N. Zheng *et al.*, “An analytical model of the knee for estimation of internal forces during exercise”, *Journal of biomechanics*, vol. 31, no. 10, pp. 963–967, 1998.
- [43] J. Victor *et al.*, “The influence of muscle load on tibiofemoral knee kinematics”, *Journal of orthopaedic research*, vol. 28, no. 4, pp. 419–428, 2010.
- [44] M. Wünschel *et al.*, “Gender differences in tibiofemoral kinematics and quadriceps muscle force during weight-bearing knee flexion in vitro”, *Knee Surgery, Sports Traumatology, Arthroscopy*, vol. 21, no. 11, pp. 2557–2563, 2013.
- [45] L. P. Maletsky *et al.*, “Accuracy of an optical active-marker system to track the relative motion of rigid bodies”, *Journal of biomechanics*, vol. 40, no. 3, pp. 682–685, 2007.
- [46] (2005 - 2015). Atlas of knee MRI anatomy, [Online]. Available: <http://w-radiology.com/knee-mri.php>.
- [47] E. Isaza *et al.*, “Determination of mechanic resistance of osseous element through finite element modeling”, in *Proceedings of the 2013 COMSOL Conference in Boston*, 2013.
- [48] H. Kurosawa *et al.*, “Simultaneous measurement of changes in length of the cruciate ligaments during knee motion.”, *Clinical orthopaedics and related research*, vol. 265, pp. 233–240, 1991.
- [49] S. B. Cohen *et al.*, “MRI measurement of the 2 bundles of the normal anterior cruciate ligament”, *Orthopedics*, vol. 32, no. 9, 2009.
- [50] F. K. Fuss, “Anatomy of the cruciate ligaments and their function in extension and flexion of the human knee joint”, *Developmental Dynamics*, vol. 184, no. 2, pp. 165–176, 1989.
- [51] R. Jones *et al.*, “Mechanical properties of the human anterior cruciate ligament”, *Clinical Biomechanics*, vol. 10, no. 7, pp. 339–344, 1995.
- [52] J. H. Yoo *et al.*, “The geometry of patella and patellar tendon measured on knee MRI”, *Surgical and radiologic anatomy*, vol. 29, no. 8, pp. 623–628, 2007.
- [53] J. L. Baldwin and C. K. House, “Anatomic dimensions of the patella measured during total knee arthroplasty”, *The Journal of arthroplasty*, vol. 20, no. 2, pp. 250–257, 2005.
- [54] A. Schmitz *et al.*, “The measurement of in vivo joint angles during a squat using a single camera markerless motion capture system as compared to a marker based system”, *Gait & posture*, vol. 41, no. 2, pp. 694–698, 2015.
- [55] M. Lafortune *et al.*, “Three-dimensional kinematics of the human knee during walking”, *Journal of biomechanics*, vol. 25, no. 4, pp. 347–357, 1992.
- [56] P. A. Costigan *et al.*, “Knee and hip kinetics during normal stair climbing”, *Gait & posture*, vol. 16, no. 1, pp. 31–37, 2002.
- [57] J. L. Krevolin *et al.*, “Moment arm of the patellar tendon in the human knee”, *Journal of biomechanics*, vol. 37, no. 5, pp. 785–788, 2004.
- [58] J. Fulkerson and D. Buuck, *Disorders of the Patellofemoral Joint*. Lippincott Williams & Wilkins, 2004, 4th edition, pp. 27–28, ISBN: 9780781740814.
- [59] K. B. Shelburne *et al.*, “Effect of muscle compensation on knee instability during ACL-deficient gait”, *Medicine & Science in Sports & Exercise*, vol. 37, no. 4, pp. 642–648, 2005.
- [60] A. Zeighami *et al.*, “Tibio-femoral joint contact in healthy and osteoarthritic knees during quasi-static squat: A bi-planar x-ray analysis”, *Journal of Biomechanics*, vol. 53, pp. 178–184, 2017.
- [61] J. M. Scarvell *et al.*, “Evaluation of a method to map tibiofemoral contact points in the normal knee using MRI”, *Journal of Orthopaedic Research*, vol. 22, no. 4, pp. 788–793, 2004.
- [62] B. C. Fleming and B. D. Beynnon, “In vivo measurement of ligament/tendon strains and forces: A review”, *Annals of biomedical engineering*, vol. 32, no. 3, pp. 318–328, 2004.
- [63] O. C. Brantigan and A. F. Voshell, “The mechanics of the ligaments and menisci of the knee joint”, *JBJS*, vol. 23, no. 1, pp. 44–66, 1941.
- [64] D. L. Butler *et al.*, “Location-dependent variations in the material properties of the anterior cruciate ligament”, *Journal of Biomechanics*, vol. 25, no. 5, pp. 511–518, 1992.
- [65] L. Maletsky *et al.*, “In vitro experimental testing of the human knee: A concise review”, *The journal of knee surgery*, vol. 29, no. 02, pp. 138–148, 2016.
- [66] B. C. Fleming *et al.*, “The effects of compressive load and knee joint torque on peak anterior cruciate ligament strains”, *The American journal of sports medicine*, vol. 31, no. 5, pp. 701–707, 2003.
- [67] M. K. Kwan *et al.*, “On the viscoelastic properties of the anteromedial bundle of the anterior cruciate ligament”, *Journal of biomechanics*, vol. 26, no. 4-5, pp. 447–452, 1993.